Boundary-Layer Meteorol (2014) 151:119–138
DOI 10.1007/s10546-013-9869-z

ARTICLE

Air–Sea CO_2 Gas Transfer Velocity in a Shallow Estuary

Eva Thorborg Mørk · Lise Lotte Sørensen · Bjarne Jensen · Mikael K. Sejr

Received: 16 January 2013 / Accepted: 3 October 2013 / Published online: 7 January 2014
© Springer Science+Business Media Dordrecht 2013

Abstract The air–sea transfer velocity of CO_2 (k_{CO_2}) was investigated in a shallow estuary in March to July 2012, using eddy-covariance measurements of CO_2 fluxes and measured air–sea CO_2 partial-pressure differences. A data evaluation method that eliminates data by nine rejection criteria in order to heighten parametrization certainty is proposed. We tested the data evaluation method by comparing two datasets: one derived using quality criteria related solely to the eddy-covariance method, and the other derived using quality criteria based on both eddy-covariance and cospectral peak methods. The best parametrization of transfer velocity normalized to a Schmidt number of 600 (k_{600}) was determined to be: $k_{600} = 0.3\,U_{10}{}^{2.5}$ where U_{10} is the wind speed in m s^{-1} at 10 m; k_{600} is based on CO_2 fluxes calculated by the eddy-covariance method and including the cospectral peak method criteria. At low wind speeds, the transfer velocity in the shallow water estuary was lower than in other coastal waters, possibly a symptom of low tidal amplitude leading to low intensity water turbulence. High transfer velocities were recorded above wind speeds of 5 m s^{-1}, believed to be caused

E. T. Mørk (✉)
Department of Bioscience, Aarhus University, Frederiksborgvej 399, 4000 Roskilde, Denmark
e-mail: etj@dmu.dk

L. L. Sørensen · B. Jensen
Department of Environmental Science, Aarhus University, Frederiksborgvej 399, 4000 Roskilde, Denmark
e-mail: lls@dmu.dk

B. Jensen
e-mail: bj@dmu.dk

L. L. Sørensen · M. K. Sejr
Department of Bioscience, Arctic Research Centre, Aarhus University, C.F. Møllers Allé 8, 8000 Aarhus C, Denmark

M. K. Sejr
Department of Bioscience, Aarhus University, Vejlsøvej 25, 8600 Silkeborg, Denmark
e-mail: mse@dmu.dk

by early-breaking waves and the large fetch (6.5 km) of the estuary. These findings indicate that turbulence in both air and water influences the transfer velocity.

Keywords Air–sea CO_2 exchange · Cospectral peak method · Eddy covariance · Estuaries · Transfer velocity

1 Introduction

The influence of the global oceans on the carbon cycle is of great importance to modelling the atmospheric accumulation of CO_2, and a better understanding of air–sea CO_2 exchange is likely to reduce the uncertainty in global climate models (Olsen et al. 2005; McGillis and Wanninkhof 2006; Takahashi et al. 2009).

Coastal waters represent only 7–8 % of the global ocean area but are biogeochemically very active systems and account for 14–30 % of global marine primary production (Alvarez et al. 1999; Borges et al. 2004a). Coastal waters, and especially estuaries, are often omitted from global carbon models. However, Frankignoulle et al. (1998), Borges et al. (2006) and Cai (2011) have shown that the CO_2 exchange in estuaries is an important component of the global carbon cycle, counterbalancing CO_2 uptake in continental shelves.

Air–sea exchange of CO_2 can be parametrized as,

$$F_{CO_2} = k_{CO_2}\ K\ (\Delta pCO_2) \tag{1}$$

where, F_{CO_2} is the corrected air–sea CO_2 flux, k_{CO_2} is the transfer velocity, K is the solubility of CO_2, and ΔpCO_2 is the difference between the partial pressure of CO_2 in the water and in the atmosphere (Weiss 1974; Wanninkhof et al. 2009).

ΔpCO_2 and K can be determined with relatively high precision, and it is thought that the greatest uncertainty when modelling the air–sea flux is the parametrization of k_{CO_2}. For example, the estimated global air–sea flux increases by 70 % when using the parametrization of Wanninkhof and McGillis (1999) as opposed to that proposed by Wanninkhof (1992) (Rutgersson et al. 2008). In coastal areas, the uncertainty in k_{CO_2} is even higher (Borges et al. 2004a; Rutgersson et al. 2008).

The transfer velocity is often parametrized as a function of wind speed, but it is also known to be affected by fetch, water currents, wave state, atmospheric stability, sea spray, surface films and rain (Upstill-Goddard and Frost 1999; Wanninkhof et al. 2009). Although earlier studies have tried to construct functions that include multiple parameters, the influence of the wave field still needs further validation, and this may lead to a more precise parametrization of the transfer velocity (Fangohr and Woolf 2007; Wanninkhof et al. 2009). Other studies indicate that the magnitude of k_{CO_2} is determined by turbulence in both the air and the water, making water-side convection and mixed-layer depth important controlling factors (Rutgersson and Smedman 2010; Rutgersson et al. 2011; Read et al. 2012).

Coastal waters are often more turbulent than open oceans because of increased bottom stress. Thus the exchange coefficient is likely to be larger for these waters than for the open oceans. On the other hand, it is argued that the air–sea exchange of gas in coastal waters is reduced by extra biological surface films and shorter fetch (Marino and Howarth 1993; Raymond et al. 2000; Borges et al. 2004a).

The large discrepancy in the transfer-velocity parametrizations could be explained by uncertainties in transfer-velocity measurements. The eddy-covariance method, hereafter the EC method, is considered to be the most direct method to determine the CO_2 flux used for determining transfer velocities. This method is challenging as it requires high frequency, high

precision measurement of atmospheric gas concentrations and the correction of measured fluxes for the influences of water vapour and temperature. At sea, measurements of turbulent velocity can be influenced by platform motion, whilst local airflow can be distorted by the set-up platform or vessel (Fairall and Larsen 1986; Wanninkhof et al. 2009; Griessbaum et al. 2010).

In the present work the aim is to obtain a reliable parametrization of the air–sea CO_2 gas transfer velocity for a shallow water estuary. The transfer velocities are determined from measurements of ΔpCO_2 and the turbulent flux of CO_2, with data filtered in order to increase the quality of the dataset. The transfer velocity is parametrized as a function of wind speed or the closely related friction velocity u_* to account for both turbulence and sea state (Wanninkhof et al. 2009) furthermore it is based on two datasets. One dataset using fluxes determined solely with the EC method, and a second dataset applying quality criteria from the cospectral peak method, hereafter the CSP method (Sørensen and Larsen 2010). The reported transfer velocities are compared to earlier work, and possible explanations are offered to account for the observed differences.

2 Sampling and Analytical Methods

2.1 Location and Measuring Period

pCO_2, CO_2 fluxes and meteorological data were collected from March to July 2012 in the inner part of Roskilde Fjord (Fig. 1) (55°41.5N; 12°4.92E). Roskilde Fjord is situated in the northern part of Zealand, Denmark, and flows into the Kattegat through the Isefjord. It is a semi-closed water area throughout which seawater mixes with fresh water from rivers and land to yield a salinity of 7–19 ‰. Roskilde Fjord can therefore be categorized as an estuary (Conley et al. 2000). The northern and southern parts of the estuary are separated by a low threshold that results in a long residence time of the water in the southern part (Flindt et al. 1997; Fauser et al. 2009). Roskilde Fjord can have markedly heterogeneous waters (Flindt et al. 1997); thus, the collected data only represent the inner part of the estuary known as Roskilde Bredning (Table 1).

2.2 Partial Pressure of CO_2 in the Air

Air is sampled continuously from the pier sketched in Fig. 2 and the concentration of CO_2(C) is determined using a Licor LI-6262 CO_2/H_2O closed path infrared analyzer. The concentration and partial pressure of CO_2 are calculated using relations from the manufacturer's instruction guide. The air intake is placed above the pier, 2 m from the edge, and air is sampled for 10 min every half hour. Between each sample of air, nitrogen is sampled for 5 min. It is assumed that the air above the water surface is well mixed, both horizontally and vertically, and this assumption was tested during a cruise in October 2012 measuring air pCO_2 with the PP Systems EGM-4 Environmental gas monitor for CO_2, finding heterogeneity of ± 4 ppm at the entire Roskilde Fjord (data not shown).

2.3 Partial Pressure of CO_2 in the Water

To establish pCO_2 in the water in Roskilde Bredning, a buoy with a water intake 0.2 m below the water surface was anchored 10 m from the edge of the pier (Fig. 2). It is assumed that the water is homogenous, thus the water at the buoy represents the surface water in the

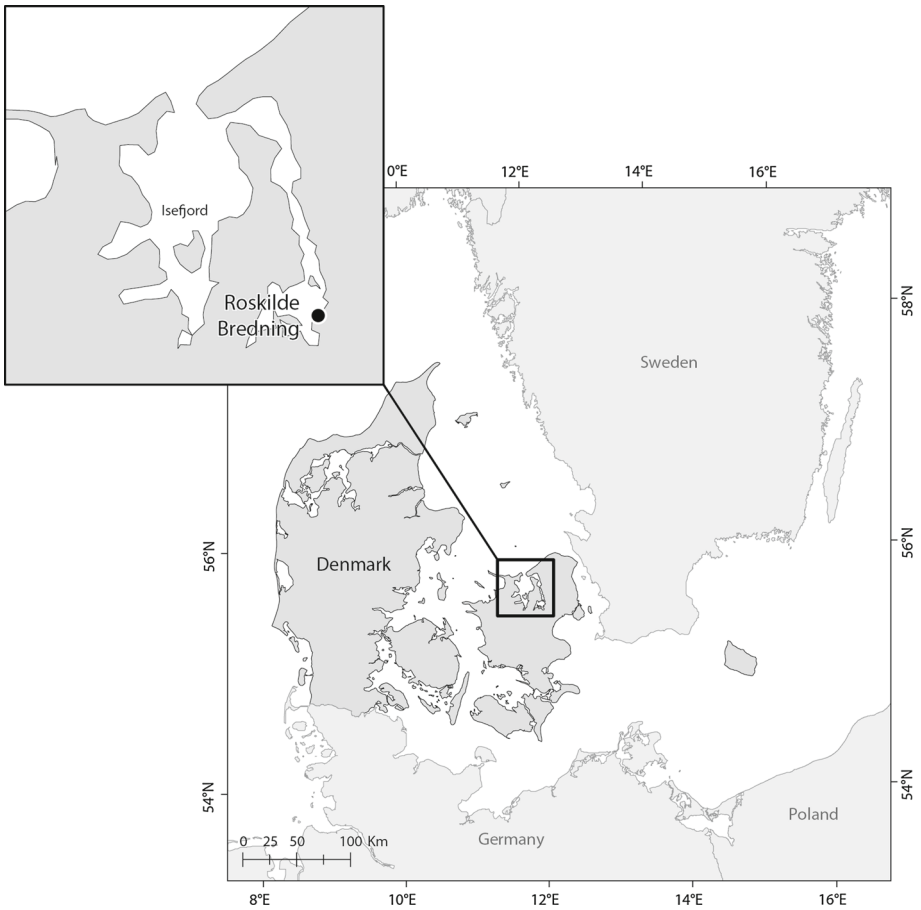

Fig. 1 Map of the study site in Roskilde Fjord, Denmark. The *black dot marks* the location of the pier from which data were collected

Table 1 Physical data for Roskilde Fjord and Roskilde Bredning (Flindt et al. 1997; Clarke et al. 2003; Fauser et al. 2009; DMI 2011)

	Roskilde Fjord	Roskilde Bredning
Surface area (km^2)	125	48
Mean water depth (m)	3	3
Mean salinity (‰)	14	10
Tidal amplitude (m)	±0.2	±0.1
Mean width (km)	≈3	≈6.5
Mean year temperature (°C)	≈8	≈8

source area of the measured CO_2 flux. The homogeneity was tested in April and July 2012; at both times a difference of $\approx \pm 10$ µatm was recorded between the water area at the pier and a water area 2 km north-west of the pier. If such heterogeneity existed during the entire measuring period, the uncertainty of ΔpCO_2 is estimated to be approximately 2 %. This uncertainty could increase during periods with a larger salinity gradient caused by intruding sea water or a high amount of run-off water from land. Furthermore a heterogeneous benthic

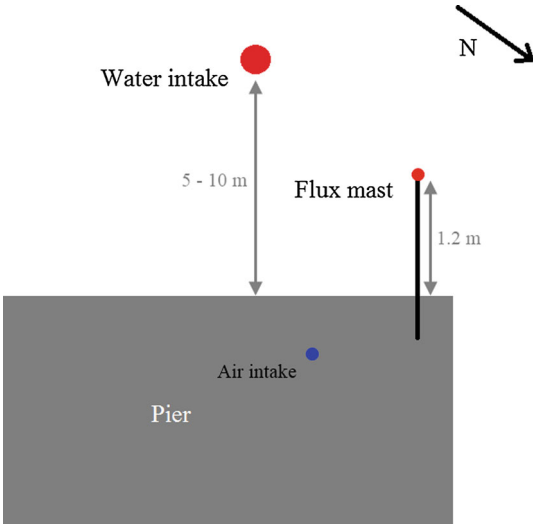

Fig. 2 Top-down view of the instrumental set-up at the pier in Roskilde Bredning. The *larger red dot* marks the water intake for pCO_2 sampling. The *black line* on the flux mast is the supporting boom. The *smaller dot* on the flux mast marks the location of the sonic anemometer and CO_2 sensor, and the *blue dot* on the pier marks the air intake for the air pCO_2

community with patches of e.g. eelgrass could create a larger spatial variation of water pCO_2 (Polsenaere et al. 2012).

At the pier, water for pCO_2 measurements was pumped continuously through an insulated water hose into a shower-head equilibrator at a flow rate of between 70 and 120 l h^{-1} (see Hilligsøe et al. (2011) and Sejr et al. (2011) for details of the instrument design). Shower-head equilibrators reach equilibrium in a short amount of time and have low uncertainty (Bakker et al. 1997; Bates et al. 1998).

For 10 min once every half-hour, the air from the equilibrator is dried and analyzed in the same infrared analyzer (LI-6262) as was used for the atmospheric pCO_2. After every 10 min of sampling equilibrated air, a sample of nitrogen follows to secure a consistent reference level.

2.4 CO_2 Fluxes Using Eddy-Covariance and Cospectral Peak Methods

The EC method was employed for measuring air–sea CO_2 fluxes. To increase the reliability of the calculated transfer velocity, the CSP method introduced by Sørensen and Larsen (2010) is used to identify and eliminate periods with potentially problematic CO_2 fluxes.

The EC method is the most common direct method for measuring gas fluxes (Fairall et al. 2000). Fluxes are determined by correlating the turbulent fluctuations of a scalar concentration with the turbulent fluctuations of the vertical wind velocity. The flux of e.g. CO_2 is then derived as

$$F_{CO_2} = \overline{w'\rho_c'} + \overline{w}\,\overline{\rho_c} \tag{2}$$

where w is the vertical wind component, ρ_c is the mass density of CO_2, the overbar denotes the mean, and the primes represent the deviation from the mean (Sørensen and Larsen 2010).

Flow distortion and platform movement influence the flux when using the EC method. To rectify this shortcoming, additional flux methods have been introduced: the inertial dissipation method (Fairall and Larsen 1986) and the CSP method (Sørensen and Larsen 2010). In the present study, the cospectra are analyzed according to the CSP method since the inertial dissipation method is sensitive to the choice of the Kolmogorov constant (Sørensen and Larsen 2010). The basic assumption of the CSP method is that a universal form for the

cospectrum exists, and that the full integral, given the covariance, can be derived from the integral of a limited spectral range (Sørensen and Larsen 2010).

When investigating the flux of a scalar quantity e.g. CO_2 (C), the flux can be estimated as

$$\overline{w'C'} \approx \frac{1}{0.25} n Co_{wC}(n)_{\text{peak}} \tag{3}$$

for $0.01 \leq$ normalized frequency (f) ≤ 0.2 using the normalized cospectrum $n\,Co_{wC}(n)$, with n being the frequency (Hz) (Sørensen and Larsen 2010), where the location of the peak is a function of stability (Norman et al. 2012) and where $f = nz/U$. In the present study, the CSP method is used to validate the $w'C'$ cospectra according to the universal spectrum presented by Kaimal et al. (1972) and Sørensen and Larsen (2010). The peak location in the frequency interval 0.01–0.2 Hz and peak magnitude of 0.25 in each sample's cospectrum determine whether or not the sample needs to be eliminated.

On a mast at a pier in Roskilde Bredning, a horizontal boom with a three-dimensional sonic anemometer, Metek USA-1, and a CO_2 sensor, the LI-7500 open-path CO_2/H_2O analyzer, is mounted, reaching 1.2 m out across the water side. The sonic anemometer operates at a sampling rate of 20 Hz, and the LI-7500 determines mass density of CO_2 and water vapour at the same frequency. The sensors are placed horizontally 0.5 m apart and 5 m above the average water level.

The fluxes used in this study are calculated using EddyPro 4.0.0 (2012) followed by post-processing of binned cospectra, where all spectral samples are averaged in exponentially-spaced frequency bins. The selected processing options and methods are shown in Appendix.

The calculated fluxes are based on half-hour sampling.

2.5 Meteorological Parameters

The Obukhov stability parameter (z/L) is calculated from

$$L = \frac{-T_{\text{p}} {u_*}^3}{\kappa g \frac{H_0}{\rho_{\text{a}} c_{\text{p}}}} \tag{4}$$

where z denotes the measurement height and L is the Obukhov length, and where T_{p} is the potential temperature, κ is the von Karman constant ≈ 0.41, g is the acceleration due to gravity ($\approx$9.81 m s^{-1}), H_0 is the uncorrected ambient sensible heat flux, ρ_{a} is moist air density and c_{p} is moist air heat capacity.

Here u_* is determined according to

$$u_* = \left(\left(\overline{u'w'} \right)^2 + \left(\overline{v'w'} \right)^2 \right)^{1/4}, \tag{5}$$

where $\overline{u'w'}$ and $\overline{v'w'}$ are the components of the kinematic momentum flux in the along-wind and in the cross-wind direction, respectively.

Wind speed is measured at 5 m (U_5), however k is commonly parametrized as a function of the wind speed at 10 m (U_{10}), thus U_{10} is calculated using the integrated Businger–Dyer relationships (Stull 1988),

$$U_z = \frac{u_*}{\kappa} \left[\ln \left(\frac{z}{z_0} \right) - \Psi_M \left(\frac{z}{L} \right) \right] \tag{6a}$$

during stable conditions

$$\Psi_M \left(\frac{z}{L} \right) = -4.7 \left(\frac{z}{L} \right) \tag{6b}$$

or during unstable conditions

$$\Psi_M\left(\frac{z}{L}\right) = 2\ln\left[\frac{(1+x)}{2}\right] + \ln\left[\frac{\left(1+x^2\right)}{2}\right] - 2\tan^{-1}(x) + \left(\frac{\pi}{2}\right) \tag{6c}$$

where

$$x = \left[1 - \left(15\frac{z}{L}\right)\right]^{1/4}. \tag{6d}$$

Here, Ψ_M is the integrated form of the dimensionless wind shear, ϕ_m, U_z is wind speed at height z and z_0 is the aerodynamic roughness length (Businger et al. 1971). This is calculated using the traditional approach based on sonic-measured wind speed at 5 m (U_5), u_* and the calculated z/L. The measuring height from sea level to the sensors varies with up to 1.5 m depending on tide, waves and amount of water held back by the wind. The maximum change of U_{10} caused by this sea level change is equal to ± 0.25 m s^{-1} and is not taken into account.

2.6 Data Quality Control and Filtering

To ensure that only reliable CO_2 fluxes and ΔpCO_2 values are used, the dataset is refined using nine criteria listed in Table 2. Based on criterion 1, samples are eliminated if $w$or CO_2 data are missing or if the LI-7500 is clearly affected by high relative humidity or rain. Criterion 2 eliminates samples collected when airflow is from the land sector (wind direction 000°–225°), or from directions that lead to pier-induced flow distortion (wind direction 225°–250° and 290°–360°). Due to set-up limitations, this criterion eliminates a very large percentage of the samples (>70 %), however, tests have shown that if all wind directions from the water sector are included and flow distortion thereby ignored, uncertain samples are eliminated in the subsequent criteria (numbers 3–6). Samples are eliminated by criterion 3 if the calculated sample-wise sonic pitch angle exceeds 5°, indicating a change in the second rotation angle caused by the edge of the pier. The specifics of the experimental set-up when measuring EC

Table 2 The criteria used to eliminate unreliable measurements

Criterion	Elimination	Rejected samples (%) (5,836 = 100 %)	Cause
DS1			
1	No C or w data	11.7	Instr.
2	Wind direction	72.7	Set-up
3	Pitch > 5°	2.5	Set-up
4	No steady state or flux-variance similarity (flag 1 and 2)	9.7	Theor. and set-up
5	Atmospheric stability	0.0	Theor.
6	No ΔpCO_2 data	0.7	Instr. and set-up
7	$\lvert\Delta pCO_2\rvert < 30\,\mu$atm	0.0	Theor.
DS2			
8	Bad cospectrum by $f \neq [0.01;0.5]$ (Hz)	0.9	Instr. and set-up
9	Bad cospectrum by peak $\neq$ $[0.15;0.35]$ $(nCo_{wC}(n)/C_*u_*)$	0.5	Instr. and set-up

Criteria 1–7 are used in dataset 1 (DS1) and 1–9 in dataset 2 (DS2)
Instr. instrumental, *Theor.* theoretical requirements not satisfied

fluxes determines the degree of flow distortion and sonic pitch angle (Dellwik et al. 2010), and the amount of data eliminated in criteria 2 and 3 could be changed with a change of mast location or height. If samples do not pass a test of steady state and flux-variance similarity and thereby do not apply to the assumptions of eddy covariance, they are flagged according to the 0-1-2 system created by Mauder and Foken (2004), and only samples flagged 0 are retained, as required by criterion 4. The flux-variance similarity test defines how well turbulence is developed and poorly developed turbulence can be a result of set-up-induced additional mechanical turbulence. Non-stationarity can be caused by e.g. changing meteorological fields. Under stable atmospheric conditions the along-wind distance that corresponds to 90 % of the flux becomes very large (in this case modelled according to Kormann and Meixner (2001) as exceeding 5.5 km), making the assumption of homogeneity in the footprint area more unlikely. Therefore, samples are eliminated when $z/L > 0.15$ (criterion 5). Samples are eliminated by criterion 6 if the equilibrator was clogged or if ΔpCO_2 data were lacking. This problem occurs when measuring with a continuously running shower-head equilibrator (Bakker et al. 1996). Furthermore, when ΔpCO_2 is close to zero, the calculation of the transfer velocity becomes more sensitive to error, and the heterogeneity of the footprint area has a higher significance (Borges et al. 2004a). As mentioned in Sect. 2.3, the heterogeneity was $\approx \pm 10\,\mu$atm, and to reduce the effect of this, samples are eliminated if the absolute value of $\Delta pCO_2 < 30\,\mu$atm (criterion 7). A possible heterogeneity in the footprint area could e.g. be caused by a spatial heterogeneity of the benthic community (Fenchel and Glud 2000).

Criteria 8 and 9 evaluate the $w'C'$ cospectra. Samples are eliminated if the peak is not located between 0.01 and 0.5 Hz (criterion 8), as suggested by Sørensen and Larsen (2010) and Norman et al. (2012), or if the maximum of the peak is outside the interval 0.15–0.35 $nCo_{wC}(n)/C_*u_*$ (criterion 9). If these two criteria are not met the cospectrum does not agree with the universal cospectrum proposed by Kaimal et al. (1972). An example of an accepted and a rejected cospectrum are shown in Fig. 3, the peak in Fig. 3a is located as described by criteria 8 and 9, while the peak of the rejected cospectrum (Fig. 3b) is located at $f = 0.01$ with $nCo_{wC}(n)/C_*u_* = 0.6$. The deviation in the low frequency part of the cospectrum is

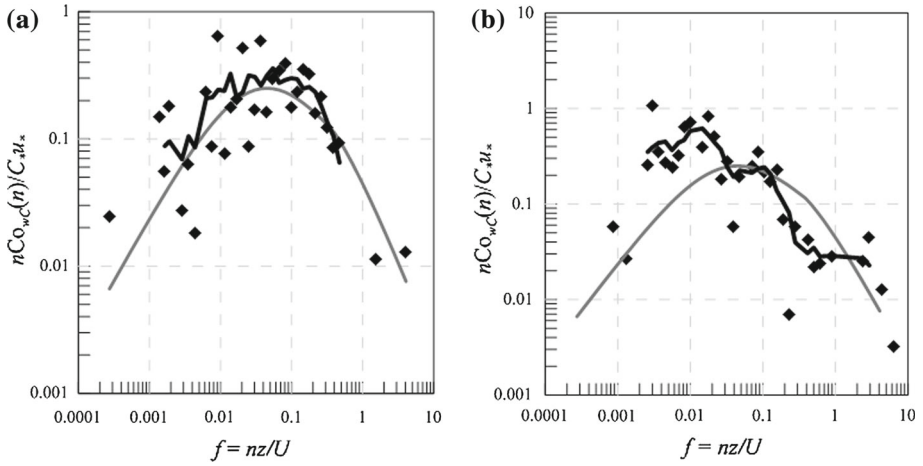

Fig. 3 Normalized $w'C'_2$ cospectra $nCo_{Cw}(n)/C_*u_*$ (*black diamonds*) plotted on logarithmic x and y axes with the running mean fit using a window width of five (*black bold line*) and the universal cospectrum suggested by Kaimal et al. (1972) (*grey line*): **a** An example of an accepted cospectrum (March 10, 2034 UTC) and **b** an example of a rejected cospectrum (March 13, 0341 UTC)

expected to be caused by flow distortion or advected gravity waves (Stull (1988)), whereas deviations in the higher frequencies are generated by white noise (El-Madany et al. 2013).

Eliminations based on criteria 1 through 7 result in a dataset (DS1) containing 157 samples (3 % of the original samples), and when adding criteria 8 and 9, a second dataset is formed (DS2) containing only 69 valid samples (1 % of the original samples) (Table 2).

To estimate the importance of using the CSP method (criteria 8 and 9) as a quality check, parametrizations of k_{CO_2} are determined based on both DS1, which is not filtered by the CSP method, and on DS2, in which a larger amount of instrumental and set-up induced error is eliminated by taking the CSP method into account.

Outliers in both datasets are ultimately eliminated by Peirce's criterion (Peirce 1852; Ross 2003). This method uses mean, standard deviation and the ratio of the maximum allowable deviation of a measured value from the mean to the standard deviation (R value) to eliminate one or several doubtful observations.

2.7 Calculation and Parametrization of CO_2 Transfer Velocity

When rearranging Eq. 1, the transfer velocity of CO_2 can be calculated as (Upstill-Goddard et al. 1990; Jacobs et al. 2002)

$$k_{CO_2} = \frac{F_{CO_2}}{K\,\Delta pCO_2} \tag{7}$$

where K is determined according to Weiss (1974). The salinity is kept at 10 ‰, and the water temperature is measured as water enters the equilibrator.

k_{CO_2} is normalized to fresh water at a temperature of 20 °C, using the Schmidt number (Sc) proposed by Wanninkhof (1992) and Raymond et al. (2000), where T is the water temperature in °C (Wanninkhof 1992; Raymond et al. 2000)

$$k_{600}/k_{CO_2} = \left(\frac{600}{Sc_{CO_2}}\right)^{-1/2}, \tag{8a}$$

$$Sc_{CO_2} = 1911.1 - (118.11\,T) + \left(3.4527\,T^2\right) - \left(0.04132\,T^3\right), \tag{8b}$$

and k_{600} is subsequently parametrized as a function of u_*, U_5 and U_{10}. As in similar studies, the parametrizations are determined by binning and averaging k_{600} in 0.05 m s^{-1} intervals for u_*, and 1 m s^{-1} intervals for U_5 and U_{10}.

3 Results

3.1 Air–Sea Transfer Velocity of CO_2 (k_{600})

k_{600} in Roskilde Bredning range from −4.89 to 1.72 mm s^{-1} with a mean and error of mean of 0.16 ± 0.5 mm s^{-1} for DS1 and −0.79 to 1.29 mm s^{-1} with a mean and error of mean of 0.24 ± 0.04 mm s^{-1} for DS2 (for comparison with earlier studies e.g. Raymond and Cole (2001) or Borges et al. (2004b) we hereafter use cm h^{-1} thus k_{600} range from −1,761 to 618 cm h^{-1} with a mean and error of mean of 59 ± 19 cm h^{-1} for DS1 and −283 to 465 cm h^{-1} with a mean and error of mean of 88 ± 14 cm h^{-1} for DS2).

Negative k_{600} is not physically possible (Borges et al. 2004b), but the samples cannot be eliminated by any of the objective quality criteria listed in Table 2. Negative k_{600} is found when H_2O fluxes are high (latent heat flux (LE) > 100 W m^{-2}), indicating that the CO_2

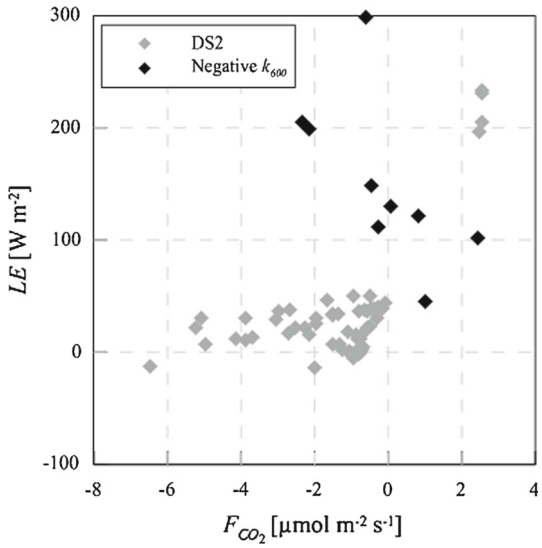

Fig. 4 Correlation between corrected CO_2 fluxes (F_{CO_2}) and latent heat fluxes (LE) in dataset 2 (DS2) with the negative transfer velocities marked

Table 3 List of calculated bin-average parametrizations of k_{600} in Roskilde Bredning

(x)	Bins	Fit	Parametrization	Name	R^2	p value
Dataset 1						
U_5	12	Power	$k_{600} = 3.1x^{1.2}$	$U_5 1$	0.51	0.045
u_*	13	Poly.	$k_{600} = -499x^2 + 544x - 62$	$u_* 1$	0.15	0.312
U_{10}	14	Linear	$k_{600} = 6.8x - 8.0$	$U_{10} 1$	0.30	0.149
Dataset 2						
U_5	6	Power	$k_{600} = 0.3x^{2.6}$	$U_5 2$	0.62	0.095
u_*	6	Power	$k_{600} = 660.3x^{2.0}$	$u_* 2$	0.91	0.007
U_{10}	8	Power	$k_{600} = 0.3x^{2.5}$	$U_{10} 2$	0.86	0.003

fluxes used to calculate the k_{600} in these cases are affected by H_2O as shown in Fig. 4. Earlier studies of air–sea CO_2 fluxes have shown a discrepancy in EC measured CO_2 fluxes due to cross correlation between CO_2 and H_2O as a result of hygroscopic particles contamination on the sensor head (Kohsiek 2000; Prytherch et al. 2010). In four samples high H_2O fluxes are not responsible for negative transfer velocities and these episodes are connected with high sensible heat fluxes ($H > 140$ W m^{-2}). The tendency is not seen in DS1, and the elimination of samples having $LE > 100$ W m^{-2} is only introduced in DS2.

The best fit in the DS1 parametrizations is a power-law regression with U_5 (Table 3). The tendency shown in Fig. 5 is for k_{600} to increase with increasing wind speed, making a linear or exponential function a reasonable regression type. The power-law fit is preferred here since it explains the greatest amount of variation in the dataset.

All three parametrizations ($U_5 1$, $U_{10} 1$ and $u_* 1$) are characterized by large scatter in the data, but the scatter is lowest in $U_5 1$ due to the binning in U_5 which eliminates, in this case, many of the negative k_{600} values as outliers. To compare $U_5 1$ with earlier work the $U_5 1$ parametrization is converted to a U_{10} parametrization, still using the bins and eliminating the outliers from $U_5 1$. This gives a parametrization based on DS1 with a $R^2 = 0.51$ and p value $= 0.045$

$$k_{600} = 2.9{U_{10}}^{1.3}. \tag{9}$$

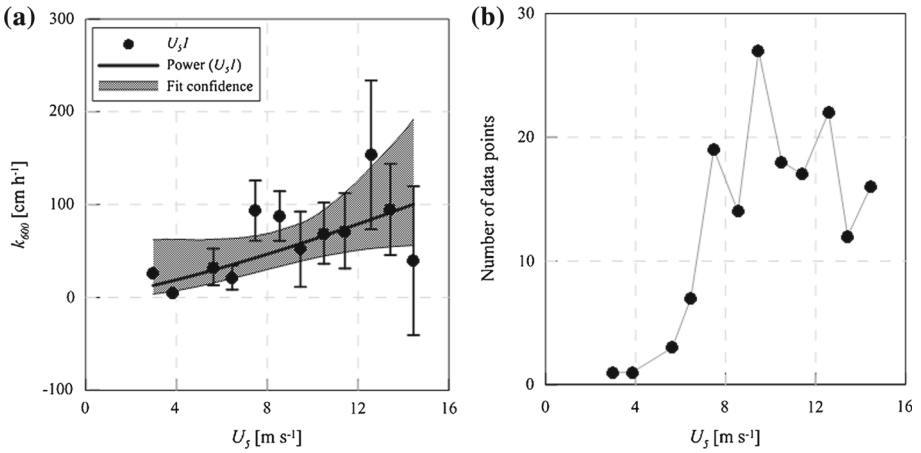

Fig. 5 **a** Parametrization of the transfer velocity of CO_2 (k_{600}) by measured wind speed at 5 m using dataset 1 ($U_5 1$). *Error bars* and *shaded area* represent the 95 % confidence level of each wind class mean and power fit, respectively. **b** Distribution of used data points

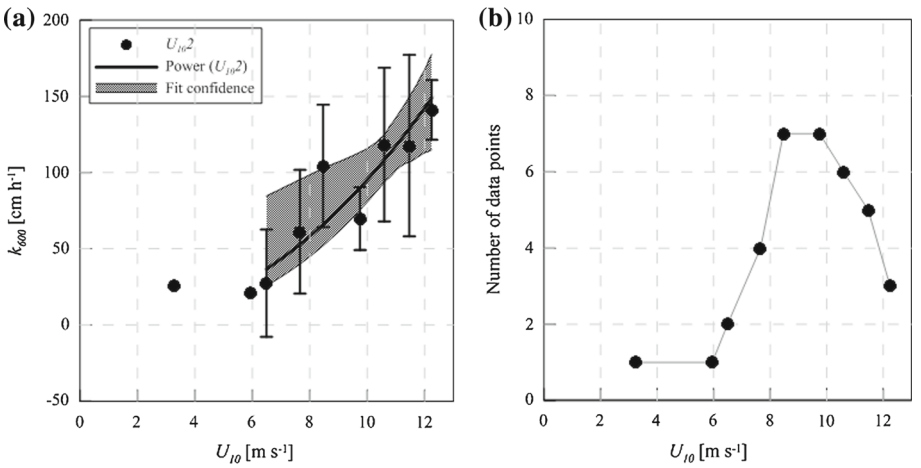

Fig. 6 **a** Parametrization of the transfer velocity of CO_2 (k_{600}) by calculated wind speed at 10 m using dataset 2 ($U_{10}2$) after the elimination of the samples with CO_2–H_2O cross-correlation and high wind speeds. *Error bars* and *shaded area* represent the 95 % confidence level of the wind-class mean and power fit, respectively. **b** Distribution of used data points

In DS2 the tendency is for k_{600} to increase with increasing wind speed until 13 m s^{-1} followed by a decrease in k_{600} from 13 to 17 m s^{-1} (data not shown), which is in direct conflict with common theory (Liss and Merlivat 1986). The low k_{600} at high wind speeds may be caused by the increased influence from sea spray and flow distortion (Wyngaard 1988; Grelle and Lindroth 1994; Griessbaum et al. 2010). Thus, the decrease of k_{600} in DS2 with increasing wind speed showed that the set-up in Roskilde Bredning can only be used at $U_{10} < 13$ m s^{-1}. With this in mind, the parametrization with the highest level of significance is given by a power function based on U_{10} inferred from u_* and measured $U_5(U_{10}2)$ as shown in Fig. 6. The parametrization in Eq. 10 gives a $R^2 = 0.86$ and $p = 0.003$

$$k_{600} = 0.3{U_{10}}^{2.5}. \tag{10}$$

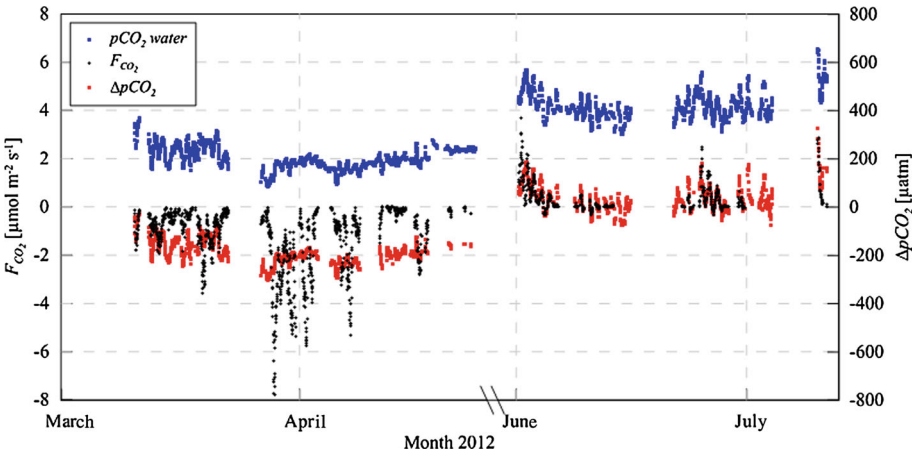

Fig. 7 Measured water pCO_2, ΔpCO_2 (the secondary y axis) and calculated CO_2 flux (F_{CO_2}) (the primary y axis) in Roskilde Bredning from March to July 2012. Data are lacking in May, thus we add a break of the x axis in this period. F_{CO_2} are calculated using Eqs. 1 and 10

$U_{10}2$ and u_*2 are very similar in R^2 and the p value, however U_{10} is once again selected instead of U_5 and u_* because it allows comparison of the results to those reported in earlier work.

The deviations in all parametrizations imply that k_{600} is not solely a function of u_* or wind speed and that experimental uncertainties or unfulfilled assumptions still exist (Jacobs et al. 1999; Nightingale et al. 2000; Weiss et al. 2007). The variability with wind speed in $U_{10}2$ is of similar size or smaller than in the studies by Raymond and Cole (2001), Weiss et al. (2007) and Borges et al. (2004b), with an R^2 of 0.53, 0.81 and 0.95, respectively. The U_{10} parametrization in Eq. 10 is therefore deemed equally solid as the three above-mentioned studies. However, it should be noted that the number of binning intervals in the present study, and thus the size of the datasets, are smaller than those employed by Weiss et al. (2007) and Borges et al. (2004b). This is due to the shorter measuring period, as well as the quality check and filtering of the data samples.

3.2 ΔpCO_2 and CO_2 Fluxes

The new parametrization of k_{600} can be used when determining the CO_2 exchange and CO_2 budget in coastal areas such as Roskilde Fjord. In the current study Eqs. 1 and 10 have been used to calculate the average CO_2 flux of Roskilde Bredning in the period for which water-side ΔpCO_2 and wind-speed data were available from March to July 2012. Figure 7 shows time series of measured water pCO_2, ΔpCO_2 and calculated CO_2 flux. Roskilde Bredning is mainly a sink of CO_2 from March to July with a mean CO_2 flux and standard deviation of the mean of -0.7 ± 0.03 µmol m^{-2} s^{-1} and ΔpCO_2 of -91 ± 2.7 µatm. It seems reasonable to conclude that the area is a CO_2 sink in the spring and early summer as indicated for similar estuaries (Algesten et al. 2004; Zemmelink et al. 2009). The CO_2 flux is equivalent to a primary production rate of approximately 269 g C m^{-2}y^{-1}, which makes the primary production in the inner part of Roskilde Fjord at the average level of other Danish estuaries (Conley et al. 2000).

The diurnal cycle of the ΔpCO_2 with the lowest values during daytime and the highest during nighttime is the opposite of that expected from temperature variations (Kuss et al.

Table 4 List of CO_2 data from studies comparable to Roskilde Bredning

Area and study	Method	Period	ΔpCO_2	CO_2 flux (μmol m^{-2} s^{-1})
Wadden Sea, DK (Zemmelink et al. 2009)	Eddy covariance	April–June 2008	−208 μatm	−2.6
Randers Fjord, DK (Borges et al. 2004a)	Chamber	April 2001	−101 to 611 ppm	−0.42 to 0.75
Baltic Sea (Norman et al. 2013)	Modelled	March–July	−90 to 0 μatm	−0.13 to 0
Scheldt, Belgian coast (Borges et al. 2004a)	Chamber	May 1998	−93 to 7,258 ppm	−0.24 to 8.8
Baltic Sea (Weiss et al. 2007)	Eddy covariance	May 2004	−87 μatm	−2.39

2006); thus, it is concluded that the variation is caused by biological production and respiration with modification from both mixing and heating/cooling.

4 Discussion

4.1 Quality and Application

ΔpCO_2 in the present study resembles data from the Baltic Sea, but it is significantly smaller than those registered in Randers Fjord, Denmark and the Scheldt off the Belgian coast (Table 4). These differences could be due to physical influences, such as longer residence time of the water, higher input of ground water and non-ventilated water from rivers in the Scheldt and Randers Fjord or different biological dynamics (Marino and Howarth 1993; Borges et al. 2006).

The mean CO_2 flux of Roskilde Bredning is less than one third of the CO_2 flux reported in the Danish Wadden Sea (Table 4), which, with regard to water depth and geographical location, is an area similar to Roskilde Fjord. The difference could be caused by the different ΔpCO_2 indicating that the Danish Wadden Sea has a higher primary production than Roskilde Bredning. However, Roskilde Bredning is a greater sink of CO_2 than both Randers Fjord or the Scheldt (Borges et al. 2004a). The discrepancy may also be due to the different experimental approach. The chamber method is known to shield the water surface, thereby preventing wind-created turbulence, resulting in smaller CO_2 fluxes (Liss and Merlivat 1986). The modelled CO_2 flux of the Baltic Sea by Norman et al. (2013) shows an uptake of CO_2, but the average of Roskilde Bredning is more than five times larger than the maximum uptake of the Baltic Sea. The CO_2 flux estimated using the EC method in the Baltic Sea in May 2004 (Weiss et al. 2007) is within the same range as Roskilde Bredning; thus, the size of the calculated CO_2 flux in the present study does not seem unrealistic for a coastal area.

The parametrizations presented in Eqs. 9 and 10 differ from those of earlier work shown in Fig. 8, however there is a large spread in the already existing parametrizations of k_{600}. Applying criteria 8 and 9 has a notable impact on the result, which would not have become apparent if only DS1 had been analyzed.

Equation 9 increases rapidly at low wind speed values, and at 4 m s^{-1}, it predicts a greater value of k_{600} than any of the other parametrizations considered. A less strong increase at low wind speeds is seen in Eq. 10; at $U_{10} > 5$ m s^{-1}, Eq. 10 shows the greatest k_{600} of all of the parametrizations, and Eq. 9 is 50 % lower at $U_{10} = 12$ m s^{-1}. Equation 10 is similar to that

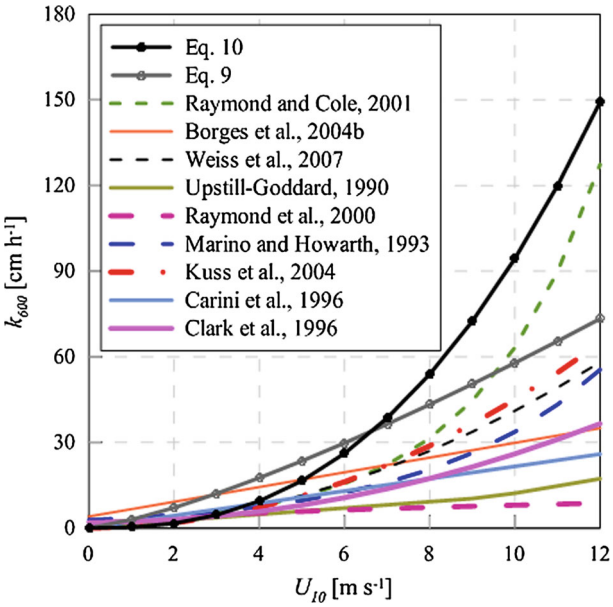

Fig. 8 Parametrizations of CO_2 transfer velocity (k_{600}) by wind speed in dataset 1 (Eq. 9) and dataset 2 (Eq. 10) compared to earlier work. The parametrizations are calculated using floating chambers (Marino and Howarth 1993; Raymond and Cole 2001; Borges et al. 2004b), eddy covariance (Weiss et al. 2007) or the deliberate and natural tracer methods (Upstill-Goddard et al. 1990; Clark et al. 1994; Carini et al. 1996; Raymond and Cole 2001; Kuss et al. 2004)

of Raymond and Cole (2001) but with a larger increase at lower wind speeds, resulting in an offset of approximately 1.5 m s^{-1} between the two parametrizations. Equation 9 from DS1 is similar to Kuss et al. (2004) or to Borges et al. (2004b), but when including the elimination based on the CSP method, it is argued that Eq. 9 overestimates the low wind speed k_{600} and greatly underestimates the high wind speed k_{600}.

The difference of Eq. 10 to the other parametrizations can both be a result of methodological or physical variations between the studies or research sites. The parametrizations shown in Fig. 8 are calculated using either floating chambers (Marino and Howarth 1993; Raymond and Cole 2001; Borges et al. 2004b), EC (Weiss et al. 2007) or the deliberate and natural tracer methods (Upstill-Goddard et al. 1990; Clark et al. 1994; Carini et al. 1996; Raymond and Cole 2001; Kuss et al. 2004). The use of floating chambers when measuring CO_2 fluxes has been shown to disturb the turbulence regime and presented limited agreement with other flux measuring methods (Broecker and Peng 1984; Belanger and Korzun 1991). Furthermore floating chambers give a snapshot in time and cover a small water-surface area (Raymond and Cole 2001). The mass-balance techniques using tracers have uncertainties caused by variations in the mixed-layer depth, shifts in wind speed over the course of the observations and difficulties accounting for the biological effect on the natural tracers (Wanninkhof et al. 2009). Although the dataset presented here is a small sample size, the CO_2 flux and ΔpCO_2 data are of high quality and exclude errors due to non-ideal conditions.

The transfer velocity is not only controlled by wind speed, and some fraction of the differences between the parametrizations may be due to the physical differences between the study sites. The earlier studies were conducted in either open water systems such as the Arkona Sea (Weiss et al. 2007) and the Baltic Sea (Kuss et al. 2004) with water depths of 45

and 27–249 m, respectively, or river systems such as the Hudson River (Marino and Howarth 1993; Clark et al. 1994) with a water depth of 14 m, width of 800 m and large influence from tidal currents. The parametrization of k_{600} in Roskilde Bredning is characterized by low k values at wind speeds <2 m s^{-1} and increasing steeply at wind speeds above 5 m s^{-1}. We speculate that this pattern could be a result of low tidal amplitude, which cause less mixing and turbulence at low wind speeds as observed in other Danish fjords (Borges et al. 2004a). The relatively large fetch combined with shallow depth could cause early wave breaking and high whitecap coverage contributing to the steep increase in k_{600} (Upstill-Goddard and Frost 1999; Nightingale et al. 2000; Borges et al. 2004a). This hypothesis was unfortunately not tested through the study period but a comparison between measured and modelled significant wave heights (H_s) in Roskilde Bredning, October 2012, showed that measured H_s are a factor of 10 smaller than the modelled H_s (using the Pierson–Moskowitz value $H_s = 0.02466{U_{10}}^2$ (Carter 1982)). The low H_s in Roskilde Bredning indicates high whitecap coverage as a result of depth-limited breaking waves (Battjes and Janssen 1978; Katsardi et al. 2012).

The CO_2–H_2O cross correlation, contaminating the measured CO_2 fluxes and thereby causing negative k_{600}, can be eliminated by application of the PKT correction (Prytherch et al. 2010), although the PKT correction can be problematic at small H_2O fluxes (Else et al. 2011; Huang et al. 2012), as during our measurement period. For these reasons it is estimated that the cross correlation is small and the PKT correction was therefore not applied to the CO_2 fluxes.

Equation 10 is a parametrization based on CO_2 flux and ΔpCO_2 data where all theoretical assumptions are attempted to be met and methodological uncertainty is minimized, and is thus proposed for application to shallow estuaries. The data screening criteria used are recommended for use in studies requiring the highest quality flux data. Criteria 8 and 9 should change with changing stability as atmospheric stability is known to change the location of the peak in the normalized cospectra (Kaimal et al. 1972; Norman et al. 2012). During stable conditions it is expected that the peak of the normalized cospectrum is located at higher frequencies than in neutral or unstable conditions (Norman et al. 2012). The importance of different stabilities was not possible to examine since the atmosphere was near neutral in the investigated period.

In future studies of the CO_2 budget concerning shallow water estuaries, Eq. 10 will give a calculated air–sea CO_2 flux resembling the actual CO_2 flux to a greater extent than earlier used parametrizations. The difficulty of choosing the correct parametrization in a shallow estuary is discussed in Zemmelink et al. (2009) and Eq. 10 would be a better choice than parametrizations based on data from rivers or the open sea.

4.2 Uncertainties

It is often difficult and expensive to measure air–sea fluxes by the EC method and many set-ups introduce flow or motion distortion (Sørensen and Larsen 2010; Griessbaum et al. 2010). Most of the motion distortion can easily be eliminated in coastal regions if measurements are conducted from a fixed platform, such as a pier, or directly from a mast mounted on the coastline. But depending on the shore line such set-ups can introduce flow distortion, which, in the present study, may result in a large number of uncertainties. The effect of the flow distortion was eliminated to the greatest extent possible, but it did not eliminate the decrease in k_{600} at high wind speed. This can only be avoided by changing the set-up at the pier.

An uncertainty introduced in most coastal areas is the water heterogeneity that can cause the measured water pCO_2 to differ from the pCO_2 in the flux footprint area. The size and location of the footprint area is dependent on atmospheric stability, wind speed and wind

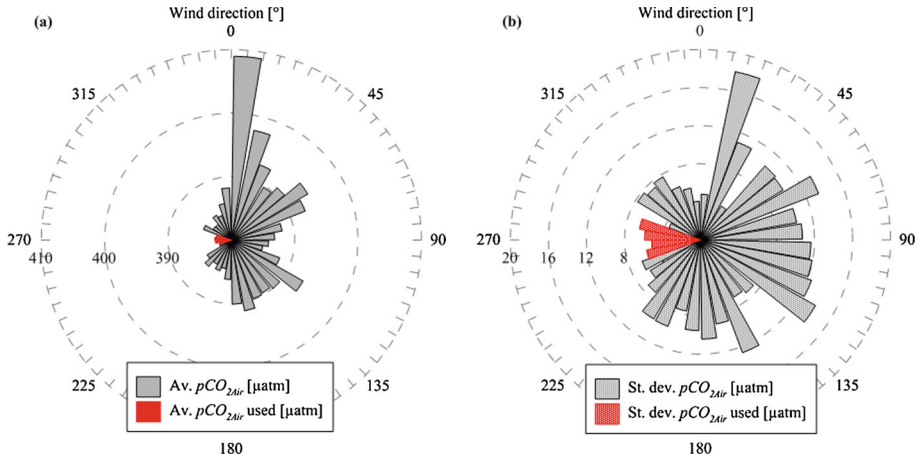

Fig. 9 Atmospheric pCO_2 (pCO_{2Air}) and wind direction in 10° wind spans where *red* represent the wind directions used to find k_{600}: **a** wind-span mean; and **b** wind-span standard deviation

direction, where stable conditions and high wind speeds lead to a larger footprint area. The water heterogeneity was investigated twice during the study period, with results that indicate very homogenous water conditions. However, the homogeneity was only examined by measurements at two points in space. Ideal conditions for determining k_{600} would be a footprint area with the highest contribution to the measured flux located at the water intake for the pCO_2 measurements. In the present study the highest contribution to the measured flux is on average located ≈130 m from the water intake as modelled according to Kormann and Meixner (2001) or Kljun et al. (2004). A heterogeneous footprint area can furthermore affect the spectra, as is seen with u and v in Murthy et al. (2009), where large eddies in the stable atmosphere have a long memory and have to travel far in homogenous terrain to reach equilibrium with the surface.

In addition to heterogeneous waters, the heterogeneous surrounding terrain at a coastal site might have an effect on the measured CO_2 flux as air masses can be advected from land (Leinweber et al. 2009). The study site is mainly surrounded by agricultural land but is located 5 km north of the city Roskilde (50,000 population), 3 km north-east of 6 km^2 forest and 200 m south-west of the research facility DTU Risø. Advected air masses from Roskilde and DTU Risø are seen in the wind directions 000°–065° and 110°–180° where the average atmospheric pCO_2 values shown in Fig. 9a are above 390 µatm. The effect of the agricultural area east of the mast can be seen by low and highly variable atmospheric pCO_2 in the wind sector from 065°–110° (Fig. 9a, b). The similar pattern in the south-east wind sector is estimated to be advected air from the forest areas. The wind directions used to calculate k_{600} are not affected by the surrounding non-water terrain, since this wind sector has a low average atmospheric pCO_2 with a low amount of variation, hence less pronounced diurnal and seasonal variations (Leinweber et al. 2009).

5 Conclusions

We estimate the air–sea transfer velocity of CO_2 in a shallow estuary (k_{600}), and present a data screening method that increases the quality of data upon which parametrizations of k_{600}

in coastal regions are based. The data screening resulted in two different datasets (DS1 and DS2) from which two different k_{600} parametrizations were derived.

Values of k_{600}, based on measurements made between March and July 2012 in an estuary (Roskilde Bredning), were generally higher than estimates reported in earlier work for coastal waters. It is proposed that these higher values of k_{600} are caused by early-breaking waves produced by the shallow water (3 m) and large fetch (6.5 km) at Roskilde Bredning. At low wind speeds, k_{600} was found to be lower than most other parametrizations, which could relate to low intensity water turbulence in the estuary unrelated to wind action (e.g. tidal currents).

The low k_{600} at low wind speeds and the rapid increase with increasing wind speed were only evident in dataset DS2. This supports the conclusion that CO_2 fluxes from which k_{600} is calculated must be critically evaluated and, if possible, complimented by a second flux method e.g. the cospectral peak method to achieve a robust parametrization. Furthermore, the sample cospectra quality control based on the cospectral peak method indicates that the set-up at the pier does not generate reliable k_{600} values at wind speeds above 13 m s^{-1}, and suggests that the physically incongruous negative k_{600} values are a result of the CO_2–H_2 O cross-correlation effect on CO_2 fluxes determined from eddy covariance.

These results suggest that the choice of parametrization, when calculating a CO_2 flux in an estuary, is of even greater importance than was previously thought. When selecting a parametrization, it is therefore necessary to ensure sufficient similarity between study sites with respect to e.g. water depth, fetch, and size of tide. This can only be achieved when parametrizations are dependent not only on wind speed, but also on additional variables.

Acknowledgments This work was part of a Ph.D. project supported by ECOCLIM, funded by The Danish Council for Strategic Research. We sincerely thank Søren William Lund and Kaj Morten Hildan for technical help in relation to mounting and maintenance of the experimental set-up and Risø DTU for making wave data available. Furthermore, we would like to thank the ECOCLIM and DEFROST Journal Club, Christina Levisen, Sara Pryor and Robert Peel for valuable comments on an earlier version of this manuscript.

Appendix

In the Advanced Mode of EddyPro 4.0.0 the settings shown in Table 5 are chosen using the listed methods.

Table 5 The chosen processing options and methods used in the calculation of CO_2 fluxes using EddyPro, version 4.0.0

Process	Method
Tilt correction	Double rotation
Detrending	Block average
Time lag compensation	Covariance maximization
Compensation for density fluctuations	WPL (Webb et al. 1980)
Fast Fourier transform—tampering window	Hamming
High-pass filtering	(Moncrieff et al. 2005)
Low-pass filtering	(Moncrieff et al. 1997)
Removal of spikes	Replaced with linear interpolation
Removal of dropouts	10 and 6 % accepted central and extreme drop outs, respectively
Quality check	0-1-2 system (Mauder and Foken 2004)

References

Algesten G, Wikner J, Sobek S, Tranvik LJ, Jansson M (2004) Seasonal variation of CO_2 saturation in the Gulf of Bothnia: indications of marine net heterotrophy. Global Biogeochem Cycles 18(4):GB4021

Alvarez M, Fernandez E, Perez FF (1999) Air–sea CO_2 fluxes in a coastal embayment affected by upwelling: physical versus biological control. Oceanol Acta 22(5):499–515

Bakker DCE, de Baar HJW, de Wilde HPJ (1996) Dissolved carbon dioxide in Dutch coastal waters. Mar Chem 55(3–4):247–263

Bakker DCE, de Baar HJW, Bathmann UV (1997) Changes of carbon dioxide in surface waters during spring in the Southern Ocean. Deep Sea Res II 44(1–2):91–127

Bates NR, Takahashi T, Chipman DW, Knap AH (1998) Variability of pCO_2 on diel to seasonal timescales in the Sargasso Sea near Bermuda. J Geophys Res 103:15567–15585

Battjes JA, Janssen JPFM (1978) Energy loss and set-up due to breaking of random waves. Coast Eng 1(16):569–587

Belanger T, Korzun E (1991) Critique of floating-dome technique for estimating reaeration rates. J Environ Eng 117(1):144–150

Borges AV, Delille B, Schiettecatte LS, Gazeau F, Abril G, Frankignoulle M (2004a) Gas transfer velocities of CO_2 in three European estuaries (Randers Fjord, Scheldt, and Thames). Limnol Oceanogr 49(5):1630–1641

Borges AV, Vanderborght JP, Schiettecatte LS, Gazeau F, Ferron-Smith S, Delille B, Frankignoulle M (2004b) Variability of the gas transfer velocity of CO_2 in a macrotidal estuary (the Scheldt). Estuaries 27(4):593–603

Borges AV, Schiettecatte LS, Abril G, Delille B, Gazeau E (2006) Carbon dioxide in European coastal waters. Estuar Coast Shelf Sci 70(3):375–387

Broecker WS, Peng T-H (1984) Gas exchange measurements in natural systems. In: Brutsaert W, Jirka GH (eds) Gas transfer at water surfaces. Reidel Publishing Co., Dordrecht, 639 pp

Businger JA, Wyngaard JC, Izumi Y, Bradley EF (1971) Flux–profile relationships in the atmospheric surface layer. J Atmos Sci 28(2):181–189

Cai WJ (2011) Estuarine and coastal ocean carbon paradox: CO_2 sinks or sites of terrestrial carbon incineration? Annu Rev Mar Sci 3:123–145

Carini S, Weston N, Hopkinson C, Tucker J, Giblin A, Vallino J (1996) Gas exchange rates in the Parker River estuary, Massachusetts. Biol Bull 191(2):333–334

Carter DJT (1982) Prediction of wave height and period for a constant wind velocity using the JONSWAP results. Ocean Eng 9(1):17–33

Clark JF, Wanninkhof R, Schlosser P, Simpson HJ (1994) Gas exchange rates in the tidal Hudson river using a dual tracer technique. Tellus B 46:274–285

Clarke A, Juggins S, Conley D (2003) A 150-year reconstruction of the history of coastal eutrophication in Roskilde Fjord, Denmark. Mar Pollu Bull 46(12):1615–1618

Conley DJ, Kaas H, Mohlenberg F, Rasmussen B, Windolf J (2000) Characteristics of Danish estuaries. Estuaries 23(6):820–837

Dellwik E, Mann J, Larsen KS (2010) Flow tilt angles near forest edges—part 1: sonic anemometry. Biogeosciences 7:1745–1757

DMI (2011) http://www.dmi.dk/dmi/index/danmark/klimanormaler.htm

El-Madany TS, Griessbaum F, Fratini G, Juang JY, Chang SC, Klemm O (2013) Comparison of sonic anemometer performance under foggy conditions. Agric For Meteorol 173:63–73

Else BGT, Papakyriakou TN, Galley RJ, Drennan WM, Miller LA, Thomas H (2011) Wintertime CO_2 fluxes in an Arctic polynya using eddy covariance: evidence for enhanced air–sea gas transfer during ice formation. J Geophys Res 116:C00G03

Fairall CW, Larsen SE (1986) Inertial-dissipation methods and turbulent fluxes at the air–ocean interface. Boundary-Layer Meteorol 34(3):287–301

Fairall CW, Hare JE, Edson JB, McGillis W (2000) Parameterization and micrometeorological measurement of air–sea gas transfer. Boundary-Layer Meteorol 96(1–2):63–105

Fangohr S, Woolf DK (2007) Application of new parameterizations of gas transfer velocity and their impact on regional and global marine CO_2 budgets. J Mar Syst 66(1–4):195–203

Fauser P, Vikelsøe J, Sørensen PB, Carlsen L (2009) Fate modelling of DEHP in Roskilde Fjord, Denmark. Environ Model Assess 14(2):209–220

Fenchel T, Glud RN (2000) Benthic primary production and O_2–CO_2 dynamics in a shallow-water sediment: spatial and temporal heterogeneity. Ophelia 53(2):159–171

Flindt MR, Kamp-Nielsen L, Marques JC, Pardal MA, Bocci M, Bendoricchio G, Salomonsen J, Nielsen SN, Jørgensen SE (1997) Description of the three shallow estuaries: Mondego River (Portugal), Roskilde Fjord (Denmark) and the Lagoon of Venice (Italy). Ecol Model 102(1):17–31

Frankignoulle M, Abril G, Borges A, Bourge I, Canon C, Delille B, Libert E, Theate JM (1998) Carbon dioxide emission from European estuaries. Science 282:434–436
Grelle A, Lindroth A (1994) Flow distortion by a solent sonic anemometer: wind tunnel calibration and its assessment for flux measurements over forest and field. J Atmos Ocean Technol 11(6):1529–1542
Griessbaum F, Moat BI, Narita Y, Yelland MJ, Klemm O (2010) Uncertainties in wind speed dependent CO_2 transfer velocities due to airflow distortion at anemometer sites on ships. Atmos Chem Phys 10(11):5123–5133
Hilligsøe KM, Richardson K, Bendtsen J, Sørensen LL, Nielsen TG, Lyngsgaard MM (2011) Linking phytoplankton community size composition with temperature, plankton food web structure and sea–air CO_2 flux. Deep Sea Res I 58:826–838
Huang Y, Song J, Wang J, Fan C (2012) Air–sea carbon-dioxide flux estimated by eddy covariance method from a buoy observation. Acta Oceanol Sin 31(6):66–71
Jacobs C, Kjeld JF, Nightingale P, Upstill-Goddard R, Larsen S, Oost W (2002) Possible errors in CO_2 air–sea transfer velocity from deliberate tracer releases and eddy covariance measurements due to near-surface concentration gradients. J Geophys Res 107:3128
Jacobs CMJ, Kohsiek W, Oost WA (1999) Air–sea fluxes and transfer velocity of CO_2 over the North Sea: results from ASGAMAGE. Tellus B 51(3):629–641
Kaimal JC, Wyngaard JC, Izumi Y, Coté OR (1972) Spectral characteristics of surface-layer turbulence. Q J R Meteorol Soc 98:563–589
Katsardi V, de Lutio L, Swan C (2012) An experimental study of large waves in intermediate and shallow water depths. Part I: wave height and crest height statistics. Coast Eng 73:43–57
Kljun N, Calanca P, Rotach MW, Schmid HP (2004) A simple parameterisation for flux footprint predictions. Boundary-Layer Meteorol 112(3):503–523
Kohsiek W (2000) Water vapor cross-sensitivity of open path H_2O/CO_2 sensors. J Atmos Ocean Technol 17(3):299–311
Kormann R, Meixner F (2001) An analytical footprint model for non-neutral stratification. Boundary-Layer Meteorol 99(2):207–224
Kuss J, Nagel K, Schneider B (2004) Evidence from the Baltic Sea for an enhanced CO_2 air–sea transfer velocity. Tellus B 56(2):175–182
Kuss J, Roeder W, Wlost KP, DeGrandpre MD (2006) Time-series of surface water CO_2 and oxygen measurements on a platform in the central Arkona Sea (Baltic Sea): Seasonality of uptake and release. Mar Chem 101(3–4):220–232
Leinweber A, Gruber N, Frenzel H, Friederich GE, Chavez FP (2009) Diurnal carbon cycling in the surface ocean and lower atmosphere of Santa Monica Bay, California. Geophys Res Lett 36(8):L08601
EddyPro 4.0.0 (2012) Eddy Covariance Processing Software, LI-COR Biosciences, LI-COR Inc., Lincoln, Nebraska, 68504, USA; Software available at: http://www.licor.com/env/products/eddy_covariance/software.html
Liss PS, Merlivat L (1986) Air–sea gas exchange rates: introduction and synthesis. In: The role of air-sea exchange in geochemical cycling. D. Reidel Publishing Company, Dordrecht, p 17
Marino R, Howarth RW (1993) Atmospheric oxygen-exchange in the Hudson River: dome measurements and comparison with other natural waters. Estuaries 16(3A):433–445
Mauder M, Foken T (2004) Documentation and instruction manual of the eddy covariance software package TK2, 45 pp
McGillis WR, Wanninkhof R (2006) Aqueous CO_2 gradients for air–sea flux estimates. Mar Chem 98(1):100–108
Moncrieff JB, Massheder JM, de Bruin H, Elbers J, Friborg T, Heusinkveld B, Kabat P, Scott S, Soegaard H, Verhoef A (1997) A system to measure surface fluxes of momentum, sensible heat, water vapour and carbon dioxide. J Hydrol 189(1–4):589–611
Moncrieff J, Clement R, Finnigan J, Meyers T (2005) Averaging, detrending, and filtering of eddy covariance time series. In: Handbook of micrometeorology. Springer, Dordrecht, p 25
Murthy BS, Latha R, Sukumaran C, Shivaji A, Sivaramakrishnan S (2009) On the influence of spatial heterogeneity on an internal boundary layer at a short fetch. J Earth Syst Sci 118(1):61–70
Nightingale PD, Liss PS, Schlosser P (2000) Measurements of air–sea gas transfer during an open ocean algal bloom. Geophys Res Lett 27(14):2117–2120
Norman M, Rutgersson A, Sørensen LL, Sahlée E (2012) Methods for estimating air–sea fluxes of CO_2 using high-frequency measurements. Boundary-Layer Meteorol 144(3):379–400
Norman M, Rutgersson A, Sahlée E (2013) Impact of improved air–sea gas transfer velocity on fluxes and water chemistry in a Baltic Sea model. J Mar Syst 111–112:175–188

Olsen A, Wanninkhof R, Trinanes JA, Johannessen T (2005) The effect of wind speed products and wind speed-gas exchange relationships on interannual variability of the air–sea CO_2 gas transfer velocity. Tellus B 57(2):95–106

Peirce B (1852) Criterion for the rejection of doubtful observations. Astron J 2:161–163

Polsenaere P, Lamaud E, Lafon V, Bonnefond J-M, Bretel P (2012) Spatial and temporal CO_2 exchanges measured by eddy covariance over a temperate intertidal flat and their relationships to net ecosystem production. Biogeosciences 9(1):249–268

Prytherch J, Yelland MJ, Pascal RW, Moat BI, Skjelvan I, Neill CC (2010) Direct measurements of the CO_2 flux over the ocean: development of a novel method. Geophys Res Lett 37:L03607

Raymond PA, Cole JJ (2001) Gas exchange in rivers and estuaries: choosing a gas transfer velocity. Estuaries 24(2):312–317

Raymond PA, Bauer JE, Cole JJ (2000) Atmospheric CO_2 evasion, dissolved inorganic carbon production, and net heterotrophy in the York River estuary. Limnol Oceanogr 45(8):1707–1717

Read JS, Hamilton DP, Desai AR, Rose KC, MacIntyre S, Lenters JD, Smyth RL, Hanson PC, Cole JJ, Staehr PA, Rusak JA, Pierson DC, Brookes JD, Laas A, Wu CH (2012) Lake-size dependency of wind shear and convection as controls on gas exchange. Geophys Res Lett 39(9):L09405

Ross SM (2003) Peirce's criterion for the elimination of suspect experimental data. J Eng Technol 20(2):38–41

Rutgersson A, Smedman A (2010) Enhanced air–sea CO_2 transfer due to water-side convection. J Mar Syst 80(1–2):125–134

Rutgersson A, Norman M, Schneider B, Pettersson H, Sahlée E (2008) The annual cycle of carbon dioxide and parameters influencing the air–sea carbon exchange in the Baltic Proper. J Mar Syst 74:381–394

Rutgersson A, Smedman A, Sahlée E (2011) Oceanic convective mixing and the impact on air–sea gas transfer velocity. Geophys Res Lett 38(2):L02602

Sejr MK, Krause-Jensen D, Rysgaard S, Sørensen LL, Christensen PB, Glud RN (2011) Air–sea flux of CO_2 in arctic coastal waters influenced by glacial melt water and sea ice. Tellus B 63(5):815–822

Sørensen LL, Larsen SE (2010) Atmosphere–surface fluxes of CO_2 using spectral techniques. Boundary-Layer Meteorol 136:59–81

Stull RB (1988) An introduction to boundary layer meteorology. Kluwer Academic, Dordrecht, 666 pp

Takahashi T, Sutherland SC, Wanninkhof R, Sweeney C, Feely RA, Chipman DW, Hales B, Friederich G, Chavez F, Sabine C, Watson A, Bakker DCE, Schuster U, Metzl N, Yoshikawa-Inoue H, Ishii M, Midorikawa T, Nojiri Y, Kortzinger A, Steinhoff T, Hoppema M, Olafsson J, Arnarson TS, Tilbrook B, Johannessen T, Olsen A, Bellerby R, Wong CS, Delille B, Bates NR, de Baar HJW (2009) Climatological mean and decadal change in surface ocean pCO_2, and net sea–air CO_2 flux over the global oceans. Deep Sea Res I 56:554–577

Upstill-Goddard RC, Frost T (1999) Air–sea gas exchange into the millennium: progress and uncertainties. Oceanogr Mar Biol Annu Rev 37:1–45

Upstill-Goddard RC, Watson AJ, Liss PS, Liddicoat MI (1990) Gas transfer velocities in lakes measured with SF_6. Tellus B 42(4):364–377

Wanninkhof R (1992) Relationship between wind speed and gas exchange over the ocean. J Geophys Res 97:7373–7382

Wanninkhof R, McGillis WR (1999) A cubic relationship between air–sea CO_2 exchange and wind speed. Geophys Res Lett 26(13):1889–1892

Wanninkhof R, Asher WE, Ho DT, Sweeney C, McGillis WR (2009) Advances in quantifying air–sea gas exchange and environmental forcing. Annu Rev Mar Sci 1:213–244

Webb EK, Pearman GI, Leuning R (1980) Correction of flux measurements for density effects due to heat and water-vapor transfer. Q J R Meteorol Soc 106(447):85–100

Weiss A, Kuss J, Peters G, Schneider B (2007) Evaluating transfer velocity–wind speed relationship using a long-term series of direct eddy correlation CO_2 flux measurements. J Mar Syst 66:130–139

Weiss RF (1974) Carbon dioxide in water and seawater: the solubility of a non-ideal gas. Mar Chem 2:203–215

Wyngaard JC (1988) The effects of probe-induced flow distortion on atmospheric turbulence measurements: extension to scalars. J Atmos Sci 45(22):3400–3412

Zemmelink H, Slagter H, Slooten C, Snoek J, Heusinkveld B, Elbers J, Bink N, Klaassen W, Philippart C, Baar H (2009) Primary production and eddy correlation measurements of CO_2 exchange over an intertidal estuary. Geophys Res Lett 36:L19606